Journal of Materials Chemistry A

Accepted Manuscript

This is an *Accepted Manuscript*, which has been through the Royal Society of Chemistry peer review process and has been accepted for publication.

Accepted Manuscripts are published online shortly after acceptance, before technical editing, formatting and proof reading. Using this free service, authors can make their results available to the community, in citable form, before we publish the edited article. We will replace this *Accepted Manuscript* with the edited and formatted *Advance Article* as soon as it is available.

You can find more information about *Accepted Manuscripts* in the Information for Authors.

Please note that technical editing may introduce minor changes to the text and/or graphics, which may alter content. The journal's standard Terms & Conditions and the Ethical guidelines still apply. In no event shall the Royal Society of Chemistry be held responsible for any errors or omissions in this *Accepted Manuscript* or any consequences arising from the use of any information it contains.

ROYAL SOCIETY OF CHEMISTRY

www.rsc.org/materialsA

Journal Name

ARTICLE

Received 00th January 20xx,

Accepted 00th January 20xx

DOI: 10.1039/x0xx00000x

www.rsc.org/

Hybrid materials from organic electronic conductors and synthetic-lignin models for charge storage application

Tomasz Rębiś†[a,b], Ting Yang Nilsson†[a], Olle Inganäs[*a]

Abstract

Homopolymers and copolymers of the monolignols syringol (S) and guaiacol (G) were prepared as well-defined lignin model compounds. Polymerisation was performed by phenol-formaldehyde condensation, also including the monomer hydroquinone (HQ) to extend the range of redox processes in these synthetic lignins (SLig). The chemical structures of the SLig samples were characterized by ^{13}C and quantitative ^{31}P NMR, and the molecular weight was monitored by size exclusion chromatography (SEC). Subsequently, SLig were incorporated into two different electron-conducting matrix – single-wall carbon nanotubes (SWNT) and polypyrrole (PPy), respectively. As a result, the hybrid materials, with a controlled amount of SWNT or with an unknown amount of PPy, were assembled and compared. The charge storage properties in the investigated materials are attributed to contributions from both the double-layer capacitance of the conducting matrix, and the Faradaic reactions provided by quinone groups immobilized to the electrodes. The results indicate a considerable improvement of charge capacity, with the synthetic lignins incorporated in the hybrid materials. With a PPy carrying S, G and HQ, better performance is obtained than has previously been obtained with lignin derivatives, showing maximum capacity of 94 mAh g^{-1}. Moreover, a low amount of electronic conductor (20 % wt. of SWNT) is adequate to perform the efficient electron communication between redox active quinones and the electrode surface, providing 72 mAh g^{-1}.

Introduction

A growing demand exists for the efficient and high charge density storage devices. Hence, the development of inexpensive, high-performance batteries or supercapacitors for large scale application is a challenge. This is essential for sustainable energy delivery for intermittent solar or wind energy sources.[1, 2] Electroactive organic compounds or polymers involving reversible redox reactions are considered promising candidates as electrode materials for charge storage devices. Among large diversity of suitable organics, those containing quinones have received

Journal of Materials Chemistry A Accepted Manuscript

Journal Name

ARTICLE

the greatest attention, since they have high theoretical capacity, high electron transfer kinetics, excellent redox reversibility and low cost.[3-5] Much work has been done on the synthesis and application of more effective quinone or carbonyl based materials for lithium-ion batteries as well as supercapacitors.[6-9] In the case of supercaps, the introduction of redox active moities into the electrode matrix is a simple strategy to enhance capacitance through the reversible Faradaic reactions.[10, 11]

Interestingly, a unlimited quantity of quinone precursors occur naturally in plants, for example in the form of biopolymers consisting of aromatic hydroxyphenolic or methoxyphenolic groups.[12] Thus, one of the most attractive source of quinones seems be lignin which is the second most abundant natural polymer, binding cellulose fibers together in plants.[13] The lignin derivatives from the pulping industry are delivered as complex polyphenols[14] with significantly varying chemical and physical properties,[15] depending on biological sources and chemical process history. The aromatic phenylpropane moieties of lignin can be converted into quinones by electrochemical redox, and thereby form an electroactive group introducing charge storage capacity in lignin.[16] The two-electron redox reaction of the quinones make lignin a material of choice to prepare energy storage systems with increased specific charge storage density. Hence, lignin derivatives have met with increasing research interest for energy storage application in recent years.[17] In order to increase the loading of quinones and retain facile electron transfer between reversible redox couples of non-conducting phenols and electrode surface, there is considerable interest in the incorporation of lignin derivatives into conducting polymer films[17,18] or different carbon materials such as multi-walled carbon nanotubes[19] or reduced graphene oxide.[20]

Our earlier research showed the charge capacity of polypyrrole to increase, from ca. 29 mAh g^{-1} to ca. 79 mAh g^{-1} at 1 A g^{-1} discharge rate, after introducing lignosulfonate in the system.[17] With other choices of lignin derivatives, lower values were obtained, as the (sub)tropical alkaline lignin/polypyrrole (Lig/PPy) system with more phenolic amount than lignosulfonate showed a lower charge capacity < 45 mAh g^{-1} at 1 A g^{-1} current.[21] Recent work on alkaline lignins report enhanced capacity with polypyrrole.[22] Adding extra quinones during formation of the hybrid material can enhance charge capacity.[23] This can also be done by adding different non-quinone redox species.[24] The complexity of polypyrrole chain configuration and conformation,[25] together with the ill-defined lignin derivatives with undefined structure[26] reactivity[27] and purity,[28,29] brought many uncertain parameters that may affect the charge capacity of the Lig/PPy system.

Herein, a series of well-defined lignin models were polymerized via phenol-formaldehyde condensation. Two of the main phenols from lignin, syringol and guaiacol, were used to mimic the natural hardwood and softwood lignin; hydroquinone was introduced to the system to extend the redox potential window and to add a quinone. The chemical structure, phenol reactivity and purity of the synthetic-lignin

Journal of Materials Chemistry A Accepted Manuscript

Journal Name

ARTICLE

(SLig) derivatives were obtained by NMR and SEC characterization. Furthermore, we demonstrate the assembly and charge storage properties of two hybrid systems: SLig/single-wall carbon nanotubes (SLig/SWNT) with a controlled amount of SWNT and SLig/polypyrrole (SLig/PPy) with an unknown amount of PPy in final material. PPy and SWNT both store charge and enable a fast electronic communication between the quinone sites of SLig and the electrode surface. In order to optimize the electrode performance of the SLig/SWNT, the mass ratio was varied in the range between 50-83 (wt%). In addition, the relationship between the chemical structure of SLig and the electrochemical properties of SLig/PPy and SLig/SWNT is also revealed. The amount of phenolic content, bonding between phenolic groups and types of phenolic groups were correlated to the electrochemical properties of the SLig/PPy and SLig/SWNT hybrid electrodes in a comparative analysis. With the best of these SLig polymers, we attain charge density values superior to the hybrids of polypyrrole and lignosulfonate.

Results and discussions

Characterization of the synthetic lignin derivatives by NMR* and *by SEC

Syringol (S), guaiacol (G) and hydroquinone (HQ) monomers were chosen to prepare synthetic lignin derivatives via condensation reaction with formaldehyde (Scheme 1). Two types of homopolymers PolyS and PolyG were synthesized by syringol (PolyS) and guaiacol (PolyG) respectively. Two types of copolymers were synthesized by copolymerizing syringol and guaiacol (PolySG); and copolymerizing syringol, guaiacol and hydroquinone (PolySGHQ). The chemical structure of the synthetic lignin derivatives were characterized by ^{1}H, ^{31}P and ^{13}C, NMR, and the molecular weights were monitored by SEC.

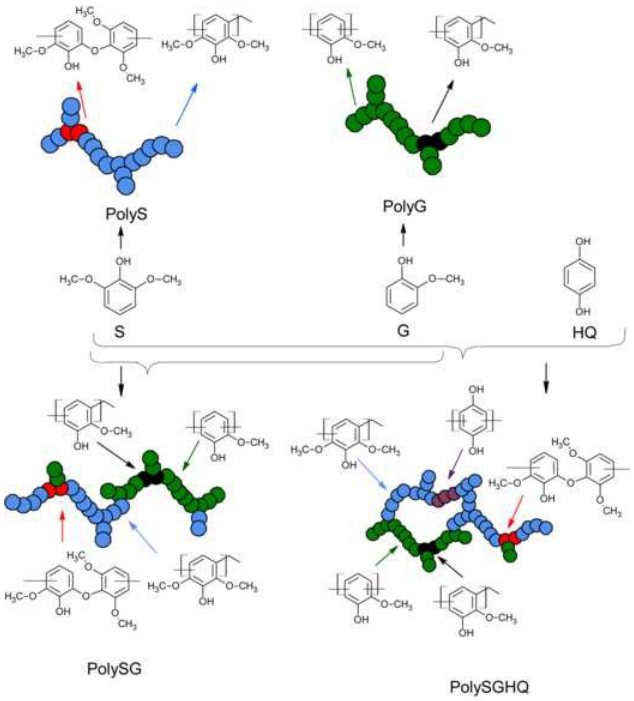

Scheme 1. Schematic representation for synthesis of synthetic lignin derivatives via phenol-formaldehyde condensation.

The hydroxyl group in the synthetic lignin derivatives were coupled with 2-chloro-4,4,5,5-tetramethyl-1,3,2-dioxaphospholane (phosphitylating reagent) and internal standard to reveal the type and amount of phenolic hydroxyl. The ^{31}P NMR spectrum in Fig. 1. a for homopolymer PolyS, show a significant peak at 142.7-143.2 ppm and a relatively small peak at 141.2-141.7

Journal of Materials Chemistry A Accepted Manuscript

Journal Name

ARTICLE

ppm, which are the spectral range of the diphenylmethane condensed and biphenyl ethers (4-O-5') condensed phenolic unit.[31] This indicate that the syringyl (S) units in PolyS were mostly condensed during the polymerization. In Fig. 1. (b), the spectrum of the other homopolymer PolyG showed relatively small peaks at 142.7-143.2 ppm and a prominent peak at 140.0-139.0 ppm, which correlate to diphenylmethane condensed phenolic and guaiacyl (G) unit. The PolyG showed much less diphenylmethane phenolic condensation and no 4-O-5' condensed compared to PolyS. In the spectrum of copolymer PolySG (Fig. 1. c), peaks are found at 142.7-143.2 ppm, 140.0-139.0 ppm, which indicate the combination of the diphenylmethane condensed and biphenyl ethers (4-O-5') condensed S unit and G unit in the copolymer. In the spectrum of the copolymer PolySGHQ (Fig. 1. d), peaks are seen at 142.7-143.2 ppm, 140.0-139.0 ppm, and 138.8-137.2 ppm, which indicate the diphenylmethane condensed, biphenyl ethers (4-O-5') condensed S unit, G unit and hydroquinone unit in the copolymer PolySGHQ.

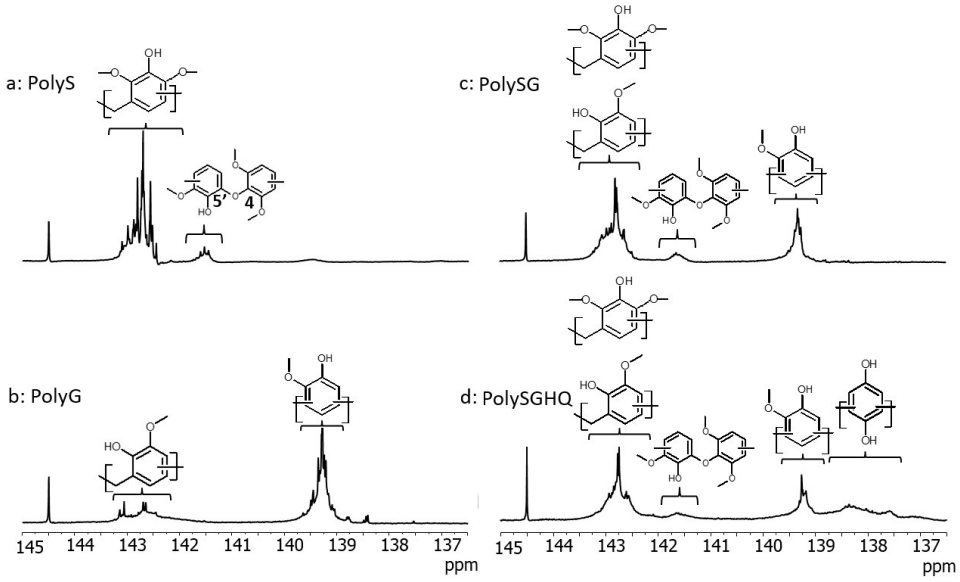

Fig. 1. ^{31}P NMR spectra of synthetic lignin derivatives. Homopolymers are (a) PolyS, (b) PolyG; and copolymers (c) PolySG and (d) PolySGHQ. The the internal standard as IS at 144.4 ppm.

The molecular weights of the homopolymers PolyS, Poly G and the copolymers Poly SG, Poly SGHQ were monitored by SEC. In Fig. 2, the SEC trace showed that the PolyS, Poly G, Poly SG and Poly SGHQ were mostly high molecular weight polymers (compared to the standard polymer passing time). This indicated the successful polymerization of the SLig via polycondensation with formaldehyde. The SEC trace of PolyS and PolyG were almost identical, the main peaks found at 22.0 to 23.8 minutes and other less significant

Journal of Materials Chemistry A Accepted Manuscript

Journal Name

ARTICLE

peaks at 23.8-24.6 minutes, at 24.6-25.0 minutes, at 25.2-25.8 minutes and at 26.5-26.8 minutes. These indicated the peak molecular weight of the PolyS at 15-19 kDa and for PolyG at 15-18.6 kDa, as well as that the distribution of the smaller molecular weight were similar. The copolymer PolySG showed main peaks at 22.0 to 23.8 minutes and peak at 24.6-25.0 minutes and the other small peak at 26.5-26.8 minutes. This indicate that the PolySG has similar peak molecular weight of 15-19 kDa and less fractions of small molecular weights, compare to the homopolymers. The copolymer PolySGHQ showed main peak at 20.9-23.8 minutes and the other peak at 24.6-25.0 minutes, which indicated the highest peak molecular weight 14.7-25.3 kDa, and much less fraction of small molecular weight, compared to the other polymers.

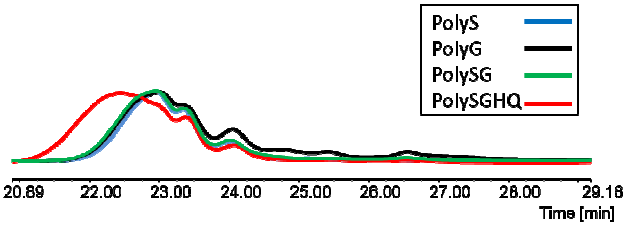

Fig. 2. SEC traces of the synthetic lignin PolyS, PolyG, Poly SG and Poly SGHQ at UV-vis 280 nm.

Probing the electrochemical properties of monolignol monomers and SLig via SWNT

The electrochemical properties of SLig were first investigated by cyclic voltammetry. In order to get more insight into the redox behavior of SLig, the monomers (guiacol and syringol) as well as ferulic acid, sinapic acid and hydroquinone, were studied for comparison as reference markers of quinone redox of SLig on single-wall carbon nanotubes. SWNT are excellent electrode materials due to their good electrical conductivity, high porosity, as well as relatively good chemical stability.[32] These properties of SWNT can be utilized to promote the electron-transfer reaction when applied as electrode materials in energy storage devices or electroanalysis. The surface of SWNT can be easily modified by noncovalent strong π-π stacking interaction between SWNT and hydrophobic electroactive molecules.[10,19] In addition, SWNT being good electronic conductors, they can act as a networks transporting electrons from the electrode surface to redox active moieties. As seen in Fig. 3, the cyclic voltammograms of the phenolics (guaiacol, syringol, ferulic acid, sinapic acid and hydroquinone) exhibit a well-defined reversible redox couples, typically observed for adsorbed functionalities with small peak-to-peak separations. Moreover, the large surface area of SWNT allows to significantly increase the surface coverage of electroactive species, thus enhancing the voltammetric signals that can be observed. On the basis of previous literature reports on molecules containing similar methoxyphenolic groups, such as capsaicine,[33] hesperidin,[34] curcumin[35,36] or eugenol,[37] it is possible to predict that the electrochemical oxidation of studied compounds leads to the development of a reversible redox couple involving o-benzoquinone/catechol moieties.

Journal of Materials Chemistry A Accepted Manuscript

Journal Name

ARTICLE

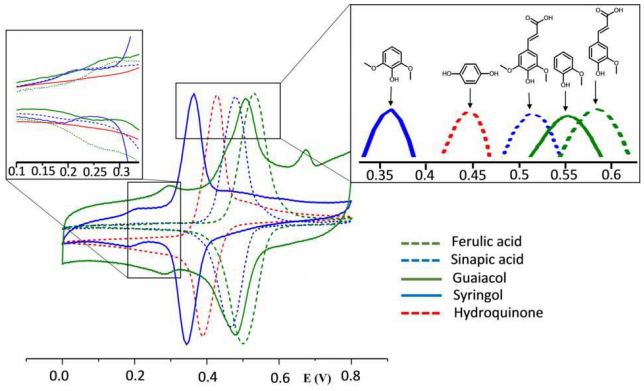

Fig. 3. Cyclic voltammograms of Ferulic acid/SWNT, Sinapic acid/SWNT, Guaiacol/SWNT, Syringol/SWNT and Hydroquinone/SWNT in 0.1 M $HClO_4$, scan rate 10 mV s^{-1}.

The oxidative demethoxylation and formation of reversible redox couple was observed during the first CV scan recorded in 0.1 M $HClO_4$ for all studied systems, with the exception of hydroquinone. Upon first scan an irreversible oxidation wave is observed at ca. 0.7 V followed by the development of a redox couple positioned at lower potentials in subsequent scans (the representative example is Ferulic acid on SWCNT which is presented in Fig. S1). This process involves the chemical step (hydrolysis) resulting in removal of methanol molecule[33,37]. Similar behavior was also observed for lignosulfonates adsorbed on a gold electrode.[16] Different numbers of oxygen containing groups substituted to the aromatic ring result in different values of $E^{0'}$ of the recorded redox signals (Fig. 3.). This phenomenon can be explained by the existence of electron donating effect arising from electron-rich oxygen atoms. Thus, the groups with a higher substitution degree produce redox couples with lower $E^{0'}$ values. This is consistent with data obtained for the studied phenolic compounds. As seen, the predominant redox couple for molecules possessing two methoxyl groups, such as syringol (1,3-dimethoxy-2-hydroxybenzene) and sinapic acid, appear at 0.35 and 0.45 V, respectively. For comparison, peaks assigned to guaiacol (2-methoxyphenol) and ferulic acid are shifted toward more positive values (0.5 V for guaiacol and 0.55 V for ferulic acid). The existence of predominant couples can be ascribed to o-benzoquinone/catechol transitions originating from *o*-methoxyphenol oxidation.[17,19] For syringol, guaiacol and ferulic acid a second reversible, minor redox couple can be seen at lower potential values (see inset Fig. 3). Low values of $E^{0'}$ suggest that peaks can derive from the additional substitution of aromatic ring by oxygen containing groups. The existence of such couples can probably be associated with the chemical reaction occurring when *o*-quinones are oxidized. Since electrogenerated *o*-quinone moieties are quite reactive and can lead to Michael adducts by nucleophilic attack, the potential assisted hydroxylation can occur in aqueous solution.[37] The $E^{0'}$ for hydroquinone is in good agreement with the data presented in literature.[38]

The synthetic lignin model with redox functions has been created by polymerization of guaiacol and syringol as well as hydroquinone. Further, the SLig/SWNT hybrid materials were assembled to create the electronic communication between redox active polymer sites and electrode surface through the highly conducting carbon nanotubes support. In order to investigate the electrochemical performance of the

Journal of Materials Chemistry A Accepted Manuscript

Journal Name

ARTICLE

SLig/SWNT hybrid materials, CV was performed in 0.1 M $HClO_4$. As seen in Fig. 4 (a) the CV profile for SWNT electrode shows a typical double-layer capacitive response with no distinctive redox peaks. In contrast, the CV of PolyG/SWNT exhibits the well-defined reversible quinone peaks at 0.48 V. The formal potential of the redox pair of PolyG/SWNT is very consistent with the position of Guaiacol/SWNT peaks (Fig. 4 b). On the other hand, the redox pair of PolyS/SWNT at 0.43 V is shifted about 80 mV towards more positive values in comparison to Syringol/SWNT studied as reference (Fig. 4 a). The observed difference may appear due partially to the existence of mixed products generated during condensation of syringol. Hence, the present electrochemical behavior of PolyS/SWNT is rather similar to Guaiacol/SWNT. As seen on Fig. 4 (c), the peaks derived from PolySG/SWNT show electroactivity at a potential between the values corresponding to that obtained for Syringol/SWNT and Guaiacol/SWNT, suggesting the influence of both components to electrochemical response. As is demonstrated in Fig. 4 (d), the PolySGHQ/SWNT hybrid material exhibit two slightly overlapping redox couples. Taking into account the electrochemical features mentioned above, the peaks recorded at 0.26 V and 0.45 V should be ascribed to hydroquinone and guaiacol/syringol electroactivity, respectively.

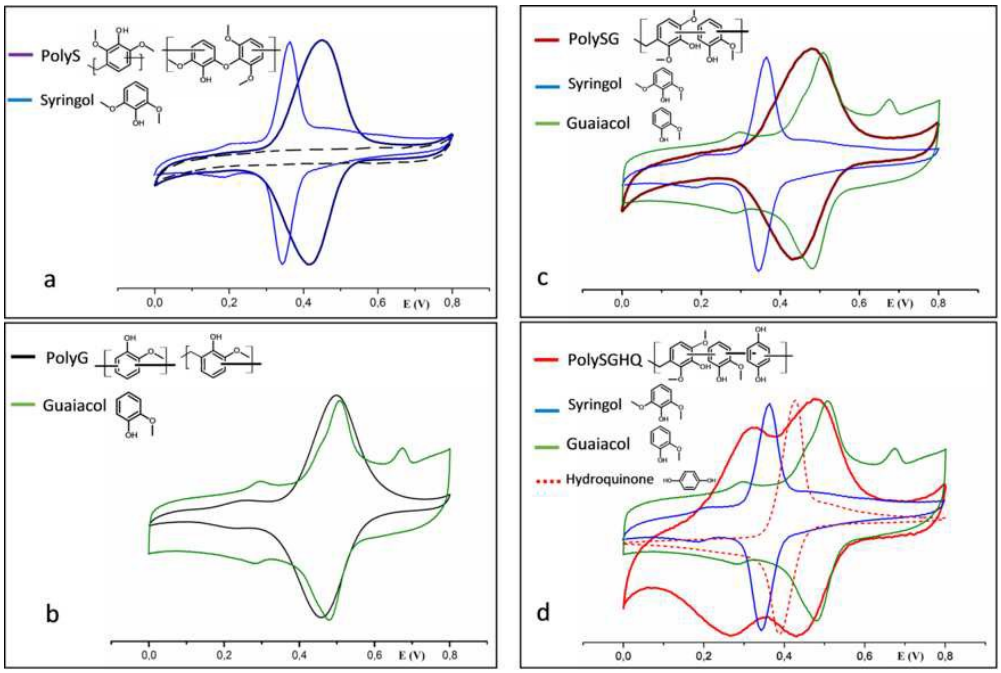

Fig. 4. Cyclic voltammograms of SLig/SWNT hybrid materials and corresponding various phenol derivatives in 0.1 M $HClO_4$ at 10 mV s^{-1}.

Journal of Materials Chemistry A Accepted Manuscript

Journal Name

ARTICLE

Electrochemical characterization of SLig/PPy hybrid electrodes

The SLig/PPy hybrid films were electrochemically synthesized from 0.1 M pyrrole and tetraethylammonium tosylate in ethylene glycol (EG) solution with the synthetic-lignin derivative PolyS, PolyG, PolySG and PolySGHQ respectively. The cyclic voltammetry was initially performed to characterize the electrochemical properties of SLig/PPy hybrid films. Upon first few cycles in an oxidative direction an activation process (demethoxylation) and creation of quinones can be observed (Fig. S2).

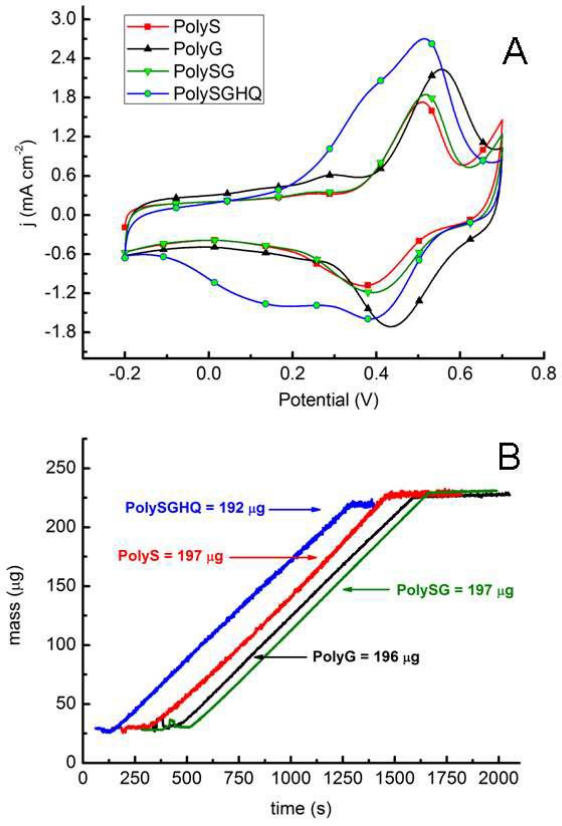

Fig. 5. Cyclic voltammograms of the PolyS, PolyG, PolySG and PolySGHQ hybrid Ppy films recorded at 1 mV s^{-1} in 0.1 M $HClO_4$. The film thickness was ca. 1 µm (A). Mass changes obtained for the electrochemical polymerization of SLig/PPy hybrid films on gold electrode (B).

The cyclic voltammograms of the different SLig/PPy hybrid films in Fig. 5 A show various contributions of redox activity. A pair of pronounced redox peaks similar to what is found for SLig/SWNT and lignosulfonate doped PPy[17] show up at ca. 0.5 V for the PolyS/PPy, PolyG/PPy and PolySG/PPy hybrid films. The formal potential of PolyG/PPy peaks at 0.49 V was the highest among the hybrid films. This value is in good agreement with that obtained for PolyG/SWNT (0.48 V). The peak-to-peak potential separation (ΔE_p) about 100 mV was measured for SLig/PPy hybrids. Therefore, when compared with SLig/SWNT, they exhibit larger ΔE_p, suggesting that charge propagation between SLig and PPy is slower than between SLig and SWNT. This may partially be due to slow diffusion of ions through the bulk of PPy electrode, which is a common drawback of conducting polymer based electrodes.[17,39] Additionally, in SLig/SWNT, π–π stacking interaction can lead to a short distance between the conjugated carbon skeleton and the redox active sites. Consequently, the conversion of quinone to hydroquinone occurs at low charge-transfer resistance and rapidly responds to the applied potential (Fig. 4). The PolyS/PPy film with mostly condensed unit and PolySG/PPy with partly condensed units show a similar redox couple at 0.44 V, which is in good correlation to PolyS/SWNT (0.43 V). For the PolySGHQ/PPy hybrid film, there were two well-pronounced, partially overlapping features; one at

Journal of Materials Chemistry A Accepted Manuscript

Journal Name

ARTICLE

ca. 0.25 V could be associated to HQ units and one at 0.44 V which could be associated to S, G and weakly bonded HQ units.[40] The mass changes during the electropolymerization of SLig/PPy films were estimated by using EQCM. As seen from the Fig. 5 B, linear mass-time profiles were recorded. All of SLig/PPy materials present a very similar mass (192-197 µg).

Charge storage properties of SLig/SWNT and SLig/PPy hybrid electrodes

The formation of SLig/SWNT hybrid is a valuable strategy to obtain synergetic effects between the redox active polymer sites and a highly conducting carbon support. Moreover, it is possible to control the SWNT fraction in final hybrid material by tailoring the mass ratio between SLig and conductive matrix. This is in contrast to galvanostatic synthesis where the content of PPy in final electrode material cannot really be controlled by optimization of the synthesis solution.[17,18] Even so, the electrosynthesis can provide an effective and convenient one-step approach to incorporation of SLig into the PPy film, though the mass ratio of both components in this case is unknown.

The charge-discharge curves of the pristine SWNT and PolySGHQ/SWNT hybrid electrodes electrodes prepared with different mass ratio is shown in Fig. 6 (a). SWNT stores charge only in an electrochemical double-layer, which has been proven by its linear charge-discharge profile. The specific charge stored in pristine SWNT is 9.4 mAh g^{-1} (56 F g^{-1}) in the studied potential range. The PolySGHQ/SWNT hybrid exhibit two plateaus in the range of 0.52-0.47 V and 0.32-0.25 V which implies a change in the mechanism towards pseudocapacitive storage. These Faradaic contributions of PolySGHQ/SWNT are attributed to the fast electrochemical redox reaction of quinones due to the immobilized polymer.

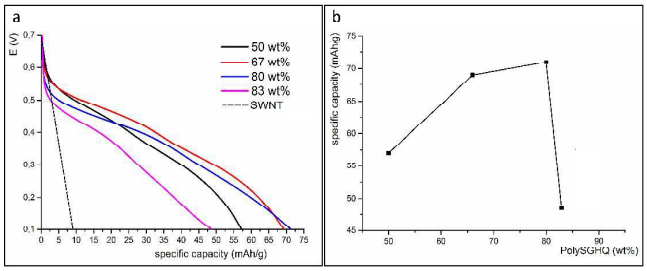

Fig. 6. Charge discharge curves for SWNT and PolySGHQ/SWNT hybrid material with different mass ratio in 0.1 $HClO_4$ at 1 A g^{-1} (a). The relationship between charge storage capacity and mass ratio between PolySGHQ and SWNT (b).

The galavanostatic charge-discharge measurements show that the Faradaic contribution delivered from synthetic lignin activity dominates in the total capacity of hybrid material. The results show that the hybrid material composed of 20 wt% of SWNTS and 80 wt% of PolySGHQ posses the highest specific charge capacity of 72 mAh g^{-1} that corresponds to 432 F g^{-1} (Fig. 6 a). The further increase of the redox polymer content above 80 wt% give rise a significant drop of specific charge capacity to 47 mAh g^{-1} (Fig. 6 b). As can be seen in Fig. 6 (b), a significant influence of the PolySGHQ content in the PolySGHQ/SWNT material on

Journal of Materials Chemistry A Accepted Manuscript

Journal Name

ARTICLE

the charge storage capacity was observed. However, this contribution cannot be analyzed within a linear model based on the SWCNT fraction. The present values of charge storage capacity for PolySGHQ/SWCNT are comparable to that previously obtained for lignin polypyrrole (75 mAh g^{-1}) composite.[17]

The charge-discharge tests of SLig/PPy hybrid films were performed at 1 A g^{-1}, (Fig. 7 A). The PPy and the SLig both contributed charge capacity in the SLig/PPy films. The phenolic amount of the PolyS, PolyG, PolySG, and PolySGHQ are collected and correlated to the specific capacity of the SLig/PPy hybrid films in Table 1. The mass ratio of SLig and pyrrole in the electrolyte used for electropolymerization was set at 1:1. However, the mass ratio in SLig/PPy is unknown.

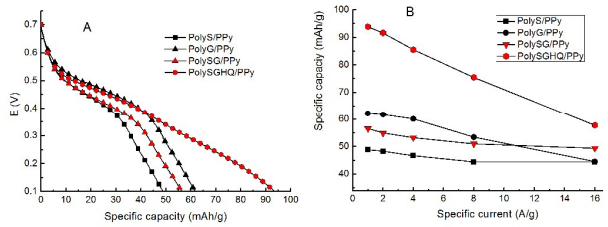

Fig. 7. Specific charge capacity at 1A g^{-1} (A) and specific capacity as a function of discharge current density (B) of the synthetic lignin derivative PolyS/PPy, PolyG/PPy, PolySG/PPy and PolySGHQ/PPy hybrid films.

At the 1A g^{-1} discharge rate, within the potential range of 0.1-0.7 V, the SLig/PPy films yielded higher specific capacity than the PPy film, which gave 30 mAh g^{-1}.[18] Similarly to the SLig/SWNT hybrids, the SLig/PPy materials exhibit a pronounced plateau region in the range of 0.55–0.40 V corresponding to reduction of quinone species. The specific charge capacity increased to 49 mAh g^{-1} (for PolyS/PPy) and 62 mAh g^{-1} (for PolyG/PPy) with increasing amount of the total phenolic groups from 15.7 mmol g^{-1} (PolyS/PPy) to 17.9 mmol g^{-1} (PolyG/PPy). The specific capacity further increased to 94 mAh g^{-1} (specific capacitance 563 F g^{-1}) for the PolySGHQ/PPy film with lower total phenolic amount in the PolySGHQ 16.4 mmol g^{-1}. This demonstrate that the charge storage capability increase with increasing amount of redox species of the S and G unit based SLig/PPy films; PolySGHQ/PPy film with HQ unit showed higher specific capacity than the S and G unit based SLig/PPy, regardless of the phenolic amount. Due to the unknown mass ratio between PPy and PolySGHQ, the causes of such improvement of charge storage in PolySGHQ are not clear. The plausible explanation may be an enhanced access to quinone moieties in PolySGHQ/PPy in comparison to PolyS/PPy and PolyG/PPy. Associated with the discharge plot in Fig. 7 A of S and G unit based SLig/PPy films, rapid decline is seen at the potential range ca. 0.35-0.10 V, where the discharge plot of PolySGHQ/PPy film showed consistent decline rate at this range. This indicated that introduction of low redox potential species (< 0.50 V) such as HQ to the model synthetic-lignin was more efficient than the increase of the phenolic amount of redox species higher than 0.50 V. The specific capacity of the SLig/PPy hybrid films at various current densities can be seen in Fig. 7 B. The specific capacity decrease at higher currents. The fastest drop of specific capacity versus current density can be observed for PolySGHQ/PPy. However, the charge storage capacity of

Journal of Materials Chemistry A Accepted Manuscript

Journal Name

ARTICLE

57 mAh g^{-1} (62%) is still obtained at high current density of 16 A g^{-1}. Furthermore, at 16 A g^{-1}, PolyG/PPy, PolyS/PPy and PolySG/PPy hold 80%, 90% and 87%, specific capacity of that at 1 A g^{-1}, respectively, suggesting a good rate capability.

Different capacitance values are obtained within the studied potential range. From the inverse of the slopes of galvanostatic discharge curves, the separated capacitances contributions from PPy and SLig can be distinguished (Fig. 8).

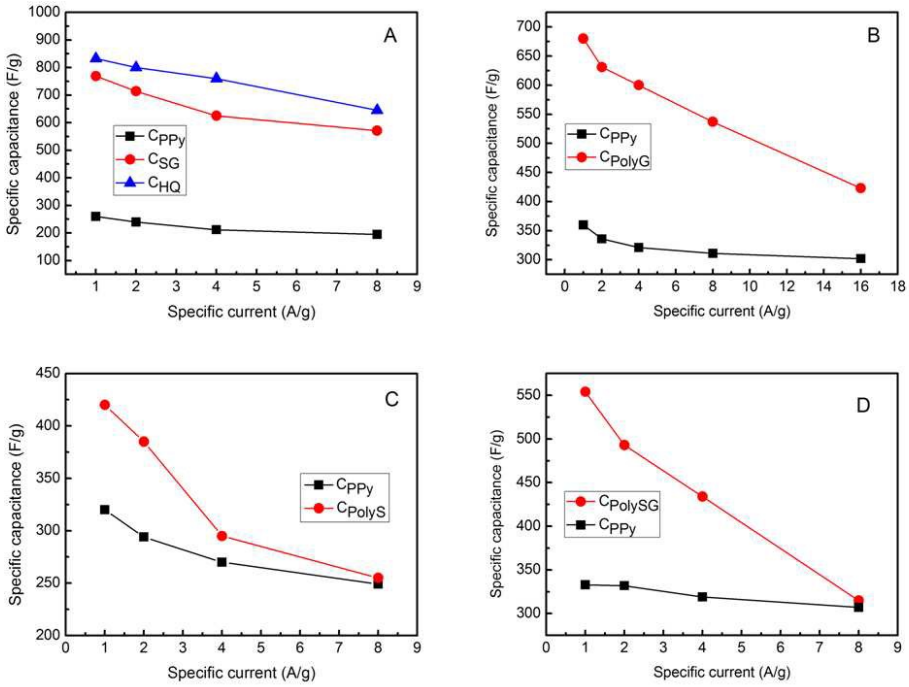

Fig. 8. Respective specific capacitance versus specific current of contributing capacitances due to PPy and quinones (SLig, HQ) of PolySGHQ/PPy (A), PolyG/PPy (B), PolyS/PPy (C) and PolySG/PPy (D) electrodes extracted from the slopes of the galvanostatic discharge curve.

HQ and SG fractions in PolySGHQ/PPy contributed to ca. 800 F g^{-1}, while PPy provided ca. 280 F g^{-1}. PolyG, PolyS and PolySG exhibited lower values of capacitances at 1 A g^{-1} (measured between 0.55-0.40 V) in comparison to PolySGHQ which is in good agreement with the CV data (Fig. 5 A). It is worth mentioning that the PPy capacitance is higher than estimated from the CV in Fig. 5 A at 1 mV s^{-1} (210 F g^{-1}). The influence of discharge rate on individual capacitances in the range of 0.55-0.40 V (quinones) is important, especially in the case of PolyG, PolyS and PolySG. Such behavior was typically observed for pseudocapacitive materials involving quinones.[17,20]

Journal of Materials Chemistry A Accepted Manuscript

Journal Name

ARTICLE

Table 1. Phenolic content and peak molecular weight of the synthetic lignin derivatives and the specific capacity of the SLig/PPy hybrid films.

Sample code	Condensed unit (mmol g^{-1}) 143.5-141.4 ppm	G unit (mmol g^{-1}) 139.6-139.0 ppm	HQ unit (mmol g^{-1}) 139.0-136.0 ppm	Redox functional groups (mmol g^{-1})	Peak molecular weight* (kDa)	Specific capacity of SLig/PPy film (-PPy) mAh g^{-1}
PPy	-	-	-	-	-	30
PolyS	15.7	-	-	15.7	14.9-19.0	49
PolyG	6.2	11.7	-	17.9	14.6-18.6	62
PolySG	11.9	4.7	-	16.6	14.7-19.0	57
PolySGHQ	8.0	3.4	5.0	16.4	14.7-25.3	94

*Peak molecular weight from RI-SEC at 22.4-23.4 minute.

Conclusions

The characteristic monolignols syringol (S) and guaiacol were used to polymerize well-defined synthetic-lignin PolyS, PolyG and PolySG via polycondensation with formaldehyde. To extend the redox potential window, hydroquinone (HQ) was introduced to the synthetic-lignin PolySGHQ as a low oxidation potential phenolic unit. The methylene bridges in the chemical structure, which were revealed by ^{13}C NMR, and the molecular weight peak over 14 kDa shown by SEC trace, confirmed the successes of the SLig derivative polymerization. The phenolic content in the SLig was measured by ^{31}P NMR. By combination with different amounts of single-wall carbon nanotubes, the correlation between the loading of electronic conductor and the charge storage capacity of the assembled SLig/SWNT hybrid material, were investigated. The charge performance of the PolySGHQ/SWNT is highest when the content of SWNT is 20 wt%. Thus, a low amount of electronic conductor (20 % wt) is adequate to provide good access to the quinones and efficient electron communication between redox active phenolics and the electrode

Journal of Materials Chemistry A Accepted Manuscript

Journal Name

ARTICLE

surface. The specific capacity was enhanced by ca. 7 times from 9.4 mAh g^{-1} (pure SWNT) to 72 mAh g^{-1} (PolySGHQ/SWNT), at current density of 1 A g^{-1}. The PolySGHQ/PPy film showed the highest specific capacity 94 mAh/g (563 F g^{-1}) after introducing the HQ unit with low oxidation potential (< 0.5 V, pH=1), where PolyG with the higher phenolic amount showed lower specific capacity 62 mAh g^{-1}. According to the results, the introduction of HQ, possessing redox potential < 0.5 V (at pH=1) enables a larger improvement of charge storage capacity for the lignin derivative/polypyrrole system. The chemical procedure highlighted here is a promising way to develop advanced electrodes for energy-storage applications from the cheap and easily accessible organic materials.

Experimental

Materials

Single-wall carbon nanotubes (SWNT) conductive aqueous ink (1 mg ml^{-1}), Dimethylformamide (DMF), pyridine, cyclohexanol, chromium (III) acetylacetonate, 2-chloro-4,4,5,5-tetramethyl-1,3,2-dioxaphospholane (phosphitylating regent), deuterated chloroform ($CDCl_3$), diethyl ether, heptane, acetone, formaldehyde water solution (37%), 2,6-dimethoxyphenol (syringol, S), 2-methoxyphenol (guaiacol, G), 4-Hydroxy-3-methoxycinnamic acid (ferulic acid), 3,5-Dimethoxy-4-hydroxycinnamic acid (sinapic acid) hydroquinone (HQ), pyrrole, tetraethylammonium tosylate, ethylene glycol (EG), perchloric acid ($HClO_4$) were purchased from Sigma-Aldrich. Pyrrole were distilled at 131°C, the other chemicals were used as received.

General procedure of polymerization of polysyringyl (PolyS) and polyguaiacyl (PolyG)

Syringol (1 g, 6.5 mmol) or guaiacol (0.81 g, 6.5 mmol) were added to formaldehyde (0.47 g, 5.9 mmol) 37 % water solution in test tubes respectively, molar ratio was set to 1 : 0.9 (phenolic monomer : formaldehyde). Oxalic acid (0.01 g, 1 wt%) was added as a catalyst. The reactions were allowed to proceed at 110 °C for 12 hours. The finished products were dissolved in EtOH and precipitated in distilled water to remove residues, and freeze-dried. The dried products were precipitated in 500 mL diethyl ether to remove the unreacted monomers, and followed by vacuum dry. The products were isolated as light brown powders. The interpretation of ^{13}C NMR (300 Hz, $CDCl_3$) spectra were based on literature[30] : PolyS δ (ppm) = 25.13-32.31 (methylene bridges: orthol ortho, paral ortho and paral para), 56.19-56.30 (-O-CH_3), 60.47 (-C-OH), 91 (hemiacetal carbons CH_3O-CH_2-OH), 118.4-120.2 (unsubstituted para carbons), 124.63-130.98 (meta carbons and substituted ortho carbons), 136.93-138.66 (substituted para carbons), 145.45-146.30 (phenoxy carbons). PolyG δ (ppm) = 31.95-41.17 (methylene bridges: orthol ortho, paral ortho and paral para), 56.00 (-O-CH_3), 111.23-121.39 (unsubstituted ortho and para carbons), 131.2-134.5 (substituted para carbons), 143.7-146.4 (phenoxy carbons). The phenolic content of the products were measured by ^{31}P NMR.

Polymerization of copolymer PolySG and PolySGHQ

Journal of Materials Chemistry A Accepted Manuscript

Journal Name

ARTICLE

PolySG: syringol (1 g, 6.5 mmol) and guaiacol (0.814 g, 6.5 mmol) at molar ratio 1:1 were added to formaldehyde (0.957 g, 11.8 mmol) 37 % water solution in test tubes respectively, phenolic monomer : formaldehyde molar ratio was set to 1 : 0.9. Oxalic acid (0.027 g, 0.1 mmol) was added as catalyst. The reactions were allowed to proceed at 110 °C for 12 hours. The finished product was dissolved in EtOH and precipitated in distilled water to remove residues and freeze-dried. The dried products were precipitated in 500 mL heptane to remove the unreacted monomers, and followed by vacuum dry. The products were isolated as light brown powder. The phenolic content of the product was measured by ^{31}P NMR.

PolySGHQ : syringol (0.349 g, 2.2 mmol), guaiacol (0.273 g, 2.2 mmol) and hydroquinone (0.242 g, 2.2 mmol) at molar ratio 1:1:1 were added to formaldehyde (0.47 g, 5.9 mmol) 37 % water solution in test tubes respectively, and the phenolic monomer : formaldehyde molar ratio was set to 1 : 0.9. Oxalic acid (0.027 g, 0.1 mmol) was added as catalyst. The reactions were allowed to proceed at 110 ◦C for 12 hours. The finished product was dissolved in EtOH and precipitated in distilled water to remove residues and freeze-dried. The dried products were precipitated in 500mL diethyl ether to remove the unreacted monomers and followed by vacuum dry. The products were isolated as light brown powder. The phenolic content of the product was measured by ^{31}P NMR.

Methods

NMR experiments were performed on a BrukerAvance 300 MHz instrument. ^{1}H NMR and ^{13}C NMR spectra were acquired at 45° pulse angle, inverse gated proton decoupling and delay time 1 second. ^{31}P NMR spectra were obtained using cyclohexanol (δ = 144.5 ppm) as an internal standard, with 90° pulse angle, inverse gated proton decoupling and delay time 2 second. The phosphitylating reagent remained and its water adduct were identified at δ = 174.7 ppm and δ = 131.8 ppm respectively. Polymer (20 mg) sample was dried in 40 °C oven overnight to remove water and then dissolved totally in 100 µl DMF. DMF/pyridine (1:1, v/v) solution 100 µl contained cyclohexanol (1.1 mg, 1.1×10^{-2} mmol) as internal standard and chromium (III) acetylacetonate (0.5 mg, 1.4×10^{-3}mmol) as relaxation agent was added subsequently. Phosphitylating regent 100µl was added to the lignin mixture and $CDCl_3$ 500 µl was then added. The final mixture was vortexed and transferred to a 5mm NMR tube for ^{31}P NMR analysis.

Size exclusion chromatography (SEC) was used for measuring the molecular weights of the lignin samples, using a 10 mM NaOH aqueous solution as the mobile phase on 3 TSK-gel columns (3000 PW, 4000 PW, 3000 PW) coupled in series. The flow rate was 1 ml/min, and detection was achieved by UV detection at 280 nm. The system was calibrated with polystyrene standards with specific molecular weights ranging from 0.342 to 805 kDa. The Millennium 2 software supplied by Waters was used to process data.

Galvanostatic polymerization of synthetic-lignin/polypyrrole (SLig/PPy) film and cyclic

Journal of Materials Chemistry A Accepted Manuscript

Journal Name

ARTICLE

voltammetry (CV) of the SLig/PPy films were performed on an Autolab PGStat 10 (EchoChemie, the Netherlands) in a three-electrode system. Lignin (16.7 mg) was totally dissolved by ultrasonication in 2.5 ml ethylene glycol with tetraethylammonium tosylate (75.4 mg, 0.1 M) as dopant and distilled. Pyrrole (16.7 mg, 0.1 M) were added to prepare 1:1 mass ratio solution. This solution was used for galvanostatic polymerization of SLig/PPy films on glassy carbon working electrode (A = 0.07 cm^{-2}) by application of constant current density (0.4 mA cm^{-2}) for 19 minutes. All the results reported in this work refer to Ag/AgCl (3 M KCl) reference electrode. The counter electrode was a platinum wire. The SLig/PPy film rinsed by distilled water, and CV was subsequently performed in 0.1M HClO4 water solution in the range of -0.2 to 0.7 V. For galvanostatic charge-discharge tests, a constant current was applied between 0.1 and 0.7 V.

Electrochemical quartz crystal microbalance (QCM Q-Sense E4) was used to measure the mass deposition on a gold quartz crystal (A = 1 cm^2) of SLig/PPy film during the galvanostatic polymerization in a three-electrode system, with Ag/AgCl as ref. electrode and platinum as counter electrode. The frequency change was monitored during the deposition at 0.4 mA cm^{-2} for 19 minutes and analyzed by the Sauerbrey equation to deduce the mass. The deposited mass of the different SLig/PPy composites on gold (A = 1 cm^2) were 197 µg (PolyS/PPy), 196 µg (PolyG/PPy), 197 µg (PolySG/PPy) and 192 µg (PolySGHQ/PPy).

The SLig/SWNT hybrid materials were prepared as follows. Single-wall carbon nanotube solution (1 mg ml^{-1}) was added to SLig ethanol solution (1 mg ml^{-1}) with four volume ratio 1:1, 2:1, 4:1 and 5:1 respectively to prepare solution with 50 wt%, 67 wt%, 80 wt% and 83 wt% of SLig. All the mixed solutions were sonicated for 10 minutes for homogeneous dispersion. Working electrodes with SLig/SWNT were prepared by drop-casting (1 µl, 1 µg) of the mixture solution on a glassy carbon electrode surface and dried properly in 60 ºC oven. The SLig/SWNT electrodes were charged and discharged respectively at 1 A g^{-1} current density at 0.1 V to 0.7 V in three electrode system containing 0.1 M $HClO_4$ supporting electrolyte. Electrochemical characterization by cyclic voltammetry was performed for the materials prepared by drop-casting (1 µl, 1 µg) of the mixed solutions (50 wt%) of SWNT and each studied compound (guaiacol, syringol, hydroquinone, ferulic acid, sinapic acid, PolyG, PolyS, PolySG, PolySGHQ).

Acknowledgments

This work was supported by the Knut and Alice Wallenberg Foundation through the project Power Papers. Dr. Michal Wagner is acknowledged by conducting some of the EQCM measurements, and discussions with colleagues in BIORGEL, Chemistry at Linköping University and KTH.

[a] *Biomolecular and Organic Electronics, IFM, Linköping University, S-581 83 Linköping. Sweden, Email:* oling@ifm.liu.se

Journal of Materials Chemistry A Accepted Manuscript

Journal Name

ARTICLE

[b] *Institute of Chemistry and Technical Electrochemistry, Faculty of Chemical Technology, Poznań University of Technology, Berdychowo 4, 60-965 Poznań, Poland*

† Tomasz Rębiś and Ting Yang Nilsson contributed equally to this work

References

1 J. Liu, J.-G. Zhang, Z. Yang, J. P. Lemmon, C. Imhoff, G. L. Graff, L. Li, J. Hu , C. Wang, J. Xiao, G. Xia, V. V. Viswanathan, S. Baskaran, V. Sprenkle, X. Li , Y. Shao, B. Schwenzer, *Adv. Funct. Mater.*, 2013, **23**, 929–946.

2 B. Huskinson, M. P. Marshak, C. Suh, S. Er, M. R. Gerhardt, C. J. Galvin, X. Chen, A. Aspuru-Guzik, R. G. Gordon, M. J. Aziz, Nature, 2014, **505**, 195–198.

3 Z. Song, H. Zhou, *Energy Environ. Sci.,* 2013, **6**, 2280–2301.

4 R. Gracia, D. Mecerreyes, *Polym. Chem.*, 2013, **4**, 2206–2214.

5 D. Vonlanthen, P. Lazarev, K. See, F. Wudl, A. J. Heeger, *Adv. Mater.*, 2014, **26,** 5095–5100.

6 X. Han, C. Chang, L. Yuan, T. Sun, J. Sun, *Adv. Mater.*, 2007, **19**, 1616–1621.

7 L. Zhao, W. Wang, A. Wang, K. Yuan, S. Chen, Y. Yang, *J. Power Sources*, 2013, **233**, 23–27.

8 T. Nokami, T. Matsuo, Y. Inatomi, N. Hojo, T. Tsukagoshi, H. Yoshizawa, A. Shimizu, H. Kuramoto, K. Komae, H. Tsuyama, J. Yoshida, *J. Am. Chem. Soc.*, 2012, **134**, 19694–19700.

9 Z. Song, H. Zhan, Y. Zhou, *Chem. Comm.*, 2009, **4**, 448–450.

10 X. Chen, H. Wang, H. Yi, X. Wang, *J. Phys. Chem. C*, 2014, **118**, 8262−8270.

11 A. Le Comte, D. Chhin, A. Gagnon, R. Retoux, T. Brousse, D. Bélanger, *J. Mater. Chem. A.*, 2015, **3**, 6146–6156.

12 C. Heitner, D. R. Dimmel, J. A. Schmidt, *Lignin and Lignans: Advances in Chemistry*, CRC Press, Boca Raton, FL 2010 .

13 S. Laurichesse, L. Avérous, *Prog. Polym. Sci.*, 2013, **39**, 1266–1290.

14 V. L. Chiang, *Environ. Chem. Lett.*, 2006, **4**, 143–146.

15 M. P. Pandey, C. S. Kim, 2011, **34**, 29–41.

16 G. Milczarek, *Langmuir*, 2009, **25**, 10345–10353.

17 G. Milczarek, O. Inganäs, *Science*, 2012, **335**, 1468–1471.

18 F. N. Ajjan, M. J. Jafari, T. Rębiś, T. Ederth, O. Inganäs, *J. Mater. Chem. A*, 2015, **3**, 12927–12937.

19 G. Milczarek, M. Nowicki, *Mater. Res. Bull.*, 2013, **48**, 4032–4038.

20 S.-K. Kim, Y. K. Kim, H. Lee, S. B. Lee, H. S. Park, *ChemSusChem*, 2014, **7**, 1094–1101.

21 S. Admassie, T. Y. Nilsson, O. Inganas, *Phys Chem. Chem. Phys.*, 2014, **16**, 24681–24684.

22 S. Leguizamon, K. P. Díaz-Orellana, J. Velez, M. C. Thies, M. E. Roberts, *J. Mater. Chem. A*, 2015, **3**, 11330–11339.

23 D. H. Nagaraju, T. Rębiś, R. Gabrielsson, A. Elfwing, G. Milczarek, O. Inganäs, *Adv. Energy Mater.*, 2013, **4**, 1–7.

Journal of Materials Chemistry A Accepted Manuscript

Journal Name

ARTICLE

24 S. Admassie, A. Elfwing, E. W. H. Jager, Q. Bao, O. Inganäs, *J. Mater. Chem. A.,* 2014, **2**, 1974–1979.

25 T. V. Vernitskaya, O. N. Efimov, *Russ. Chem. Rev*., 1997, **66**, 443–457.

26 R. Vanholme, B. Demedts, K. Morreel, J. Ralph, W. Boerjan, *Plant Physiol*., 2010, **153**, 895–905.

27 S. Shimizu, T. Yokoyama, T. Akiyama, Y. Matsumoto, *J. Agr. Food. Chem*., 2012, **60** 6471–6476.

28 K. Minu, K. K. Jiby, V. V. N. Kishore, *Biomass and Bioenergy*., 2012, **39**, 210–217.

29 A.-S. Jönsson, A.-K. Nordin, O. Wallberg, *Chem. Eng. Res. Des*., 2008, **86**, 1271–1280.

30 R. Rego, P. J. Adriaensens, R. A. Carleer, J. M. Gelan, *Polymer*., 2004, **45**, 33–38.

31 D. Argyropoulos, *J. Wood Chem. Technol*., 1994, **14**, 45–63.

32 G. G. Wildgoose, C. E. Banks, H. C. Leventis, R. G. Compton, *Microchim. Acta*, 2005, **152**, 187–214.

33 R. T. Kachoosangi, G. G. Wildgoose, R. G. Compton, *Electroanalysis*, 2008, **20**, 2495–2500.

34 M. J. Sims, Q. Li, R. T. Kachoosangi, G. G. Wildgoose, R.G. Compton, *Electrochim. Acta*, 2009, **54**, 5030–5034.

35 L. Zheng, J. Song, *Sensors Actuators B Chem*., 2009, **135**, 650–655.

36 M. A. N. Manaia, V. C. Diculescu, E. D. S. Gil, A. M. Oliveira-Brett, *J. Electroanal. Chem*., 2012, **682**, 83–89.

37 A. Ciszewski, G. Milczarek, *Electroanalysis*, 2001, **13**, 860–867.

38 H. Hong, W. Park, *Langmuir,* 2001, **17**, 2485–2492.

39 G. A. Snook, P. Kao, A. S. Best, *J. Power Sources*, 2011, **196**, 1–12.

40 M. R. Arcila-Velez, M. E. Roberts, *Chem. Mater*., 2014, **26**, 1601–1607.

Journal of Materials Chemistry A Accepted Manuscript